JOURNAL OF OPTOELECTRONICS AND ADVANCED MATERIALS Vol. 12, No. 3, March 2010, p. 427 - 431

# Deposition of chromium oxide thin films with large thermoelectromotive force coefficient by reactive pulsed laser ablation

A. P. CARICATO, A. LUCHES*, M. MARTINO, D. VALERINI, Y. V. KUDRYAVTSEV[a], A. M. KORDUBAN[a], S. A. MULENKO[a], N. T. GORBACHUK[b]
*University of Salento, Department of Physics, 73100 Lecce, Italy*
[a]*Institute for Metal Physics, NAS of Ukraine, 03142, Kiev-142, Ukraine*
[b]*Kiev State University of Technology and Design, 03011, Kiev-11, Ukraine.*

Thin films of chromium oxides were deposited on Si substrates by KrF laser ablation of a chromium target in $O_2$ atmosphere (0.05-5.0 Pa). Films exhibit semiconducting properties with band gap increasing (0.32-0.71 eV) with increasing pressure from 0.05 to 1.0 Pa. The largest values of the thermoelectromotive force coefficient *S* (~3.5-4.5 mV/K) were measured in the temperature range 270-290 K for the film deposited at 1.0 Pa. The S coefficient decreases in the same temperature range for the film deposited at lower oxygen pressures.

(Received June 21, 2009; accepted October 7, 2009)

*Keywords*: Chromium oxides, Reactive pulsed laser deposition, Nanometric films, Thermo-sensors

## 1. Introduction

Modern electronic devices require thin semiconductor films and nanometric structures with accurately tailored band gaps to get specific application. Oxides of transition metals are at present actively studied for their semiconducting, electrochromic and photochromic properties [1, 2], which depend on the band gap value, which in turn depends on the oxide stoichiometry. Chromium oxide thin films $Cr_{3-X}O_{3-Y}$ ($0 \le x \le 2$; $0 \le y \le 2$) are of great interest due to their application in solar energy converters [3], semiconductor technology [4] and spintronic heterostructures [5, 6]. Laser chemical vapour deposition of elements from $Cr(CO)_6$ carbonyl vapours [7, 8] using a nitrogen laser ($\lambda$=337 nm) was applied to synthesize chromium oxide films containing $Cr_2O_3$ and $CrO_2$ phases. This method, but using a KrF laser ($\lambda$=248 nm), was applied to synthesize chromium oxide films, too [9]. Pulsed laser deposition (PLD) was applied to grow stoichiometric $CrO_2$ on Si<111> substrates from $Cr_2O_3$ targets [10, 11]. Chromium oxide ($CrO_x$) films were also grown onto various substrates at 390 °C using KrF pulsed laser ablation of a $Cr_2O_3$ target [12]. Reactive pulsed laser deposition (RPLD) using a KrF laser ($\lambda$=248 nm) was applied to ablate $CrO_3$ and $Cr_8O_{21}$ targets in oxygen atmosphere (10-40 Pa) with the aim to deposit the $CrO_2$ phase [6] on substrates heated up to 300 °C.

RPLD technique presents some advantages for oxide film fabrication: it allows a good control of thickness and stoichiometry of deposits, by simply varying the laser pulse number and the oxygen pressure, respectively. At present, the interest is mostly for nanometric films, to test the advantages of reduced thickness in the performances of electronic devices and sensors. Our interest is the deposition of nanometric chromium oxide films with variable stoichiometry, in order to obtain semiconductor films with variable band gap. To this end, we used the RPLD technique, where a pure chromium target is ablated by energetic KrF laser pulses in a low pressure $O_2$ atmosphere. At the best of our knowledge, no reference can be found in the literature about chromium oxide films fabricated with this very simple method. In this paper, we present results on RPLD chromium oxide thin films deposition and on their electrical and electrothermal characteristics, since our aim is the use of chromium oxide films for sensor applications.

## 2. Experimental apparatus and procedure

Film depositions were performed in a stainless-steel vacuum chamber. Before each deposition the chamber was evacuated down to ~$5 \times 10^{-5}$ Pa to avoid contamination. Then, a flux of pure (99.999%) $O_2$ was introduced to obtain the desired dynamic pressure ($p$=0.05, 0.1, 1.0 and 5.0 Pa). A pure (Goodfellow, 99.5%) Cr target was ablated with KrF ($\lambda$=248 nm) excimer laser pulses at the fluence $F$=4.5 J/cm$^2$. Pulse length was ~20 ns, pulse repetition rate was 10 Hz. Each film was fabricated with 4000 consecutive laser pulses. The laser beam was incident on the target under an angle of about 45°. The target was rotated at a frequency of 3 Hz to obtain a smooth ablation procedure. Before each deposition, the target surface was cleaned using 3000 laser pulses with a shutter shielding the substrate. The ablated material was collected on <100> Si substrates. Substrates were placed at 45-mm distance

from the target. Thickness and mean composition of the deposited films were inferred from Rutherford backscattering spectrometry (RBS) with 2 MeV $He^+$ ions. The crystalline structure and composition was studied by X-ray diffraction (XRD) analysis (Cu-Kα radiation). Chemical states of chromium oxides were identified by X-ray photoelectron spectroscopy (XPS). The direct current (DC) electrical resistance of the bare Si substrate and of the Si substrate with the deposited films was measured by using the two-probe technique. Indium coatings were used for ohmic contacts. The temperature dependence of the specific conductivity ($\sigma$) of the deposited films was measured in the range 293-333 K. Calculations were made taking into account the geometrical shape of the substrate and deposits. The applied electrical field for measuring the sample electrical resistance, wherefrom $\sigma$ was calculated, was about 45 V/m. The temperature dependence of the thermoelectromotive force (thermo e.m.f.) coefficient *S* (Seebeck *S* coefficient) was also investigated. The *S* coefficient was measured with a high-resistance potentiometer after producing a thermal gradient along the sample. Ferromagnetic resonance spectra were recorded both with magnetic field *H* parallel and perpendicular to the sample surface.

## 3. Results

The thickness and mean composition of the films was inferred from computer simulation of the experimental RBS spectra. The thickness appears to increase gradually from ~50 nm to ~200 nm when the $O_2$ pressure increases from 0.05 to 1.0 Pa. Then it decreases to ~80 nm at $p$=5.0 Pa. The mean composition of films results close to $CrO_2$ at $p$=0.05 Pa, to $Cr_3O_4$ at 0.1 Pa and to $Cr_7O_8$ at higher $O_2$ pressures during depositions. It must be noticed that oxygen is a light element with consequently a low backscattering cross-section. It means that Cr/O atomic ratios are affected by errors of more than 20%.

The specific conductivity $\sigma$ of the films deposited on Si substrates presents temperature dependence typical of the semiconductor material. For instance, $\sigma$ varies from 58 $\Omega^{-1}cm^{-1}$ to 150 $\Omega^{-1}cm^{-1}$ in the temperature range 293-333 K for the sample deposited at p=0.1 Pa and from 12 $\Omega^{-1}cm^{-1}$ to 59 $\Omega^{-1}cm^{-1}$ for the sample deposited at p=1.0 Pa. The energy band gap $E_g$ of the deposited films was calculated from Arhenius plot of the ratio $\sigma(T_1)/\sigma(T)$, using he expression

$$E_g = \frac{2k \ln[\sigma(T_1)/\sigma(T)]}{1/T - 1/T_1} \qquad (1)$$

where $k$ is the Boltzmann constant, $\sigma(T_1)$ is the specific conductivity at the temperature $T_1$ and $\sigma(T)$ is the specific conductivity at the temperature $T$ ($T<T_1$). The general trend is an increase of $E_g$ with the increase of $O_2$ pressure from $p$=0.05 to $p$=1.0 Pa, while $E_g$ decreases for the sample deposited at $p$=5.0 Pa (Fig. 1).

XRD investigations show that films have a polycrystalline structure. As seen in Fig. 2, both $CrO_3$ and $Cr_2O_3$ oxides are present in the deposited films. Figure 2 also shows that the sample prepared at $p$=0.05 Pa presents a good crystalline quality, since $Cr_2O_3$ and $CrO_3$ peaks are high and narrow. Samples prepared at higher $O_2$ pressures exhibit the same peaks of the above mentioned sample, but they are lower and broader, indicating a poorer crystalline quality.

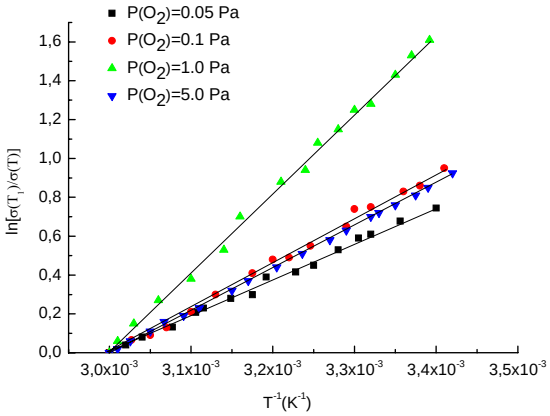


*Fig.1. Arhenius plot of ln[σ(T1)/σ(T)] vs. 1/T, wherefrom the energy band gap $E_g$ was calculated for films deposited at p=0.05 Pa: $E_g$=(0.32 ± 0.03) eV; p = 0.10 Pa:$E_g$=(0.40±0.04) eV; p=1.0 Pa: $E_g$=(0.71± 0.07) eV and p=5.0 Pa: $E_g$=(0.38± 0.04) eV.*

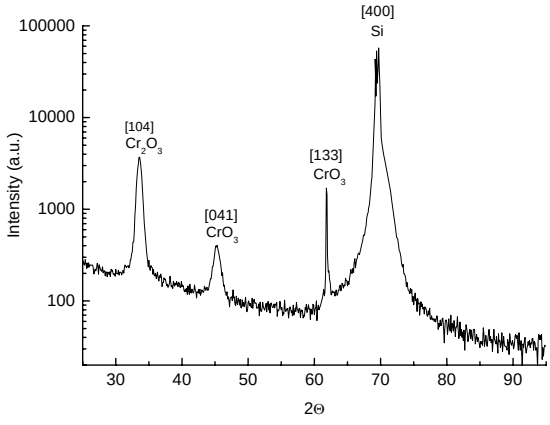


*Fig.2. XRD spectrum of the film deposited on <100> Si substrate at p=0.05 Pa.*

XPS analysis of the Cr2p fine structure shows two broad peaks around 577 eV and 586 eV, which are

attributed to $Cr2p_{3/2}$ and $Cr2p_{1/2}$, respectively (Fig.3). Experimental XPS peaks become broader as the $O_2$ pressure increases.

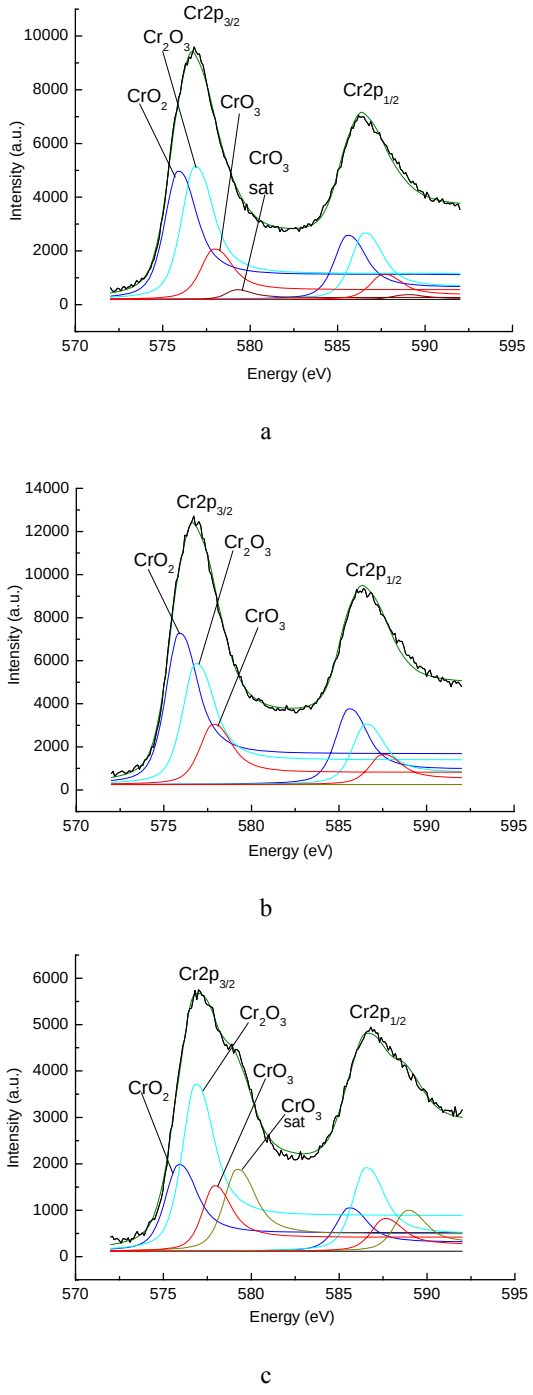


*Fig.3. Experimental XPS spectra of the $Cr2p_{3/2}$ and $Cr2p_{1/2}$ lines of the films deposited a) at p=0.1 Pa, b) at p=1.0 Pa and c) at p = 5.0 Pa and their deconvolutions.*

Computer deconvolution of the experimental spectra points to the dominant presence of the $Cr_2O_3$ chemical phases in the deposited films and to a smaller presence of the $CrO_3$ phase, like seen in the XRD spectra. A small amount of the $CrO_2$, phase has also to be considered. Its contribution becomes small in sample prepared at *p*=5.0 Pa (Fig. 3c).

Ferromagnetic resonance spectra of the films deposited on Si substrates were recorded both with magnetic field *H* parallel and perpendicular to the sample surface. Graphs of the derivative of the absorption signal are presented in Fig. 4. A small energy absorption can be observed at $H$ = 0.32 T for the sample prepared at *p*=1.0 Pa. The energy absorption at $H$ = 0.19 T is determined by the sample holder.

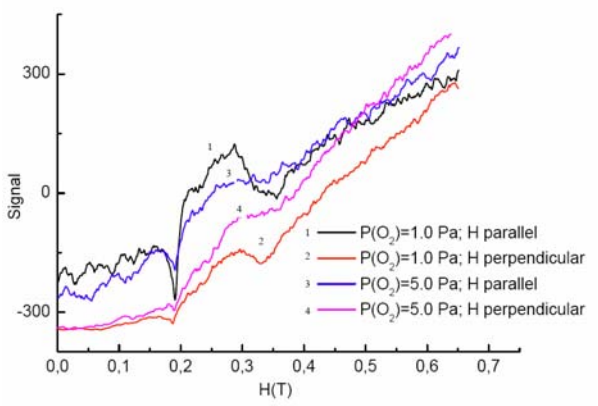


*Fig. 4. Ferromagnetic resonance spectra of films deposited at p=1.0 Pa and p=5.0 Pa. The energy absorption at $H$ = 0.19 T is determined by the sample holder.*

The trend of the thermo e.m.f. coefficient *S* vs. temperature in the range 210-333 K is presented in Fig. 5. The curves show a broad maximum (3.5-4.5 mV/K) around 285 K. The highest values of *S* were measured in the films deposited at intermediate oxygen pressures (0.10 and 1.0 Pa). The *S* coefficient is increasing up to 3.5-4.5 mV/K with increasing temperature in the range 210-285 K and then it is decreasing down to 305 K. After, one can see an increase of the *S* coefficient up to 333 K for films deposited at *p*=0.1 and 1.0 Pa, i.e. for films with the higher band gap values. From the other hand, the *S* coefficient for the films deposited at p=0.05 and 5.0 Pa, i.e. for the films with the lower $E_g$ values, is decreasing with increasing temperature in the range 280-290 K and then it is increasing up to 333 K.

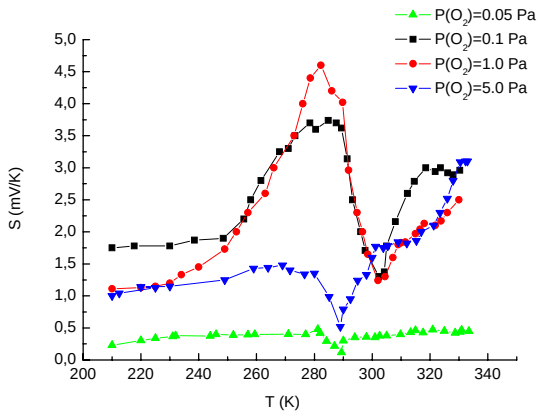


*Fig.5. Thermoelectromotive force (e.m.f.) coefficient S vs. temperature for chromium oxide films deposited at different $O_2$ pressures.*

## 4. Discussion

The shape of the Arhenius plot of electrical conductivity vs. $1/T$ is a clear evidence of the semiconducting characteristics of the deposited films. The experimental data show that the band gap $E_g$ of the semiconductor material increases with increasing oxygen pressure up to 1.0 Pa during deposition, due to the higher content of chromium oxides in films of increasing thickness. The $E_g$ values increase from 0.32 to 0.71 eV for samples prepared at $p$=0.05 Pa to samples prepared at $p$=1.0 Pa, respectively. But one can see that $E_g$ decreases to 0.38 eV for the sample prepared at p=5.0 Pa. This behaviour can be explained by the lower thickness of the film. The crystalline structure of the films can also influence $E_g$. The XRD spectra indicate that the films are polycrystalline, with crystalline quality decreasing with increasing $O_2$ pressure during depositions. It is well known that laser pulses produce an expanding plume from target to substrate where energetic atoms and ions are present [13]. The kinetic energy of the ablated species is high enough (tens of eV) to promote crystallization of the growing film, even on substrates at room temperature [14]. The interaction between the ablated material vapour and $O_2$ ambient gas leads to oxidation in the gas phase for all target materials [15]. Some contribution to oxidation can be given also by the exposition to ambient $O_2$ of the growing film. Of course, the increase of ambient pressure during ablations increases the scattering frequency of the ablated species with $O_2$ molecules and of the molecules formed in the gas phase. The effect is a decreasing of the kinetic energy of the species impinging on the substrate, with a consequent poorer crystallization of the deposits. Now, the energy gap $E_g$ depends not only on the thickness and composition, but also on the crystalline structure of films. The crystalline structure of the sample prepared at $p$=5.0 Pa is very poor and the deposited layer is essentially amorphous. Therefore, the low $E_g$ value at $p$=5.0 Pa can be attributed to the reduced thickness and amorphousness of the deposited film.

It can be noticed that the $CrO_2$ phase is present in the XPS deconvoluted spectra, but it is not present in the XRD spectra. XRD gives information on the whole film structure, while XPS only from the very surface layer, of the order of a few nm in depth. Chromium oxide $CrO_2$ phase is of interest since it is strongly ferromagnetic, but it is metastable and it easily decomposes into the antiferromagnetic $Cr_2O_3$ phase [5, 6]. Since neither XPS nor XRD measurements were performed on-line, but after exposure to air, variation of a metastable phase can be explained. Moreover, XRD technique detects crystalline phases only, while XPS records chemical bonds only. So, a limited concentration of the $CrO_2$ phase could be present in our samples, either less than the detectable limit of the XRD technique, or in an amorphous phase. From XPS spectra deconvolution it can also be seen that the higher the $Cr_2O_3$ phase concentration, the higher is the concentration of the satellite $CrO_3$ phase in the deposited films. Satellite $CrO_3$ phase appearance is caused by non coupled electrons of $Cr_2O_3$ phase. It can be seen that, when the relative concentration of this phase is low, there is no trace of the satellite phase (Fig. 3c).

Also the ferromagnetic resonance (FMR) spectra do not give the strong signal determined by the ferromagnetic $CrO_2$ phase. In fact, FMR spectra give only signal produced by paramagnetic phases. The experimental spectra are consistent with samples where there are separate $CrO_2$ ferromagnetic particles in the deposited films, which do not interact one with another. FMR spectra confirm the low $CrO_2$ phase concentration in the samples, which result formed of paramagnetic phases. As it can be seen from Fig. 4, the absorption is higher for the film with higher $CrO_2$ phase concentration, according to XPS analysis.

The thermo e.m.f. coefficient $S$ is important for studying kinetic phenomena of charge transfer in materials. To this end, it is necessary to know not only the relationship of temperature to the specific conductivity $\sigma$, but also to the $S$ coefficient. The behaviour of the thermo e.m.f. coefficient $S$ can be explained by the presence of impurities (unreacted chromium) in the semiconducting chromium oxide layer. If one takes into account the expression for electron and hole concentration of a nondegenerate semiconductor, it is possible to write $S$ in the form [16]

$$S = -\frac{k}{e}\left\{\frac{[2+\ln(N_c/n)]n\mu_n - [2+\ln(N_v/p)]p\mu_p}{n\mu_n + p\mu_p}\right\} \qquad (2)$$

where $k$ is the Boltzmann constant, $e$ is the electron charge; $n$, $p$ are electron and hole concentrations, respectively; $N_c$, $N_v$ are effective density of states in the conduction and valence bands, respectively; $\mu_n$, $\mu_p$ are electron and hole mobility, respectively. So, from equation (2) it can be seen that the thermo e.m.f. coefficient of semiconductor materials with impurities is given by two parts, which are determined by their conductive

characteristics. As it is seen from Fig. 5, the *S* coefficients depend on temperature and $E_g$ values. The largest *S* coefficient was measured for films with $E_g \approx 0.40$ and 0.71 eV. In general, the lower $E_g$, the lower are the semiconducting properties of materials and therefore the corresponding *S* coefficient is not so high. In fact, *S* coefficient is about 0.001-0.01 mV/K for metals, since the electron energy in metals does not depend practically upon temperature [16]. The *S* coefficient was reported to be ~ 0.1 mV/K at 300 K for $NaCo_2O_4$ single crystals [17]. The largest measured value of the *S* coefficient is ~ 0.41 mV/K for PbTe films deposited by thermal evaporation in vacuum [18]. In our case, the *S* coefficient has different maximum values for the various films and these values vary with temperature *T*. There are no data in literature about any thermoelectric properties of chromium oxides films.

## 5. Conclusions

RPLD was shown to be a very simple procedure for fabricating chromium oxide films: an elemental target (Cr) is ablated in a low-pressure reactive atmosphere ($O_2$). The stoichiometry and crystalline structure of the films is controlled by the $O_2$ pressure during the deposition. The film thickness is controlled by the laser pulse number and the $O_2$ pressure. The presented results show that RPLD can be used to fabricate chromium oxide layers with variable thickness, degrees of oxidation and crystallinity, and consequently with different values of their band gap $E_g$ and thermo e.m.f. coefficient *S*. This feature can allow accurate tailoring of the band gap for technological applications. The *S* coefficient was measured for chromium oxide films for the first time and it presents very high values. It means that, for instance, chromium oxide films with such high *S* coefficients can be suitable for measuring of thermochemical effect of chemical reaction (endothermal or exothermal) and to detect molecules with high oxidizing action, such as NO, CO, for instance. Finally, it is worth noting that post deposition annealing of the films is not required to promote their semiconducting characteristics.

## References

[1] Z. Hassain, J. Mater. Res. **16**, 2695 (2001).
[2] S. A. Mulenko, V. P. Mygashko, Appl. Surf. Sci. **252**, 4449 (2006).
[3] V. Moise, R. Cloots, A. Rulmont, Int. J. Inorganic Materials **3**, 1323 (2001).
[4] R. Chen, C.N. Borca, P.A. Dowben, Mat. Res. Soc. Symp. Proc. **614**, F10.1 (2000).
[5] N. Popovici, M.L. Parames, R.C. da Silva, O. Monnereau, P.M. Sousa, A. J. Silvestre, O. Conde, Appl. Phys. A **79,** 1409 (2004).
[6] D. Stanoi, G. Socol, C. Grigorescu, F. Guinneton, O. Monnereau, L. Tortet, T. Zhang, I.N. Mihailescu, Mater. Sci. Eng. B **118**, 74 (2005).
[7] F. K. Perkins, C Hwang, M.Onllion, Y.G. Kim, P. A. Dowben, Thin Solid Films **198**, 317 (1991).
[8] R. Cheng, C. N. Borca, P. A.Dowben, S. Stadler, Y. U. Idzerda, Appl. Phys. Lett. **78**, 521 (2001).
[9] P. M. Sousa, A. J. Silvestre, N. Popovici, O. Conde, Appl. Surf. Sci. **247**, 423 (2005).
[10] M. Shima, T. Tepper, C. A. Ross, J. Appl. Phys. **91**, 7920 (2002).
[11] F. Guinneton, O. Monnereau, L. Argeme, D. Stanol, G. Socol, I.N. Mihailescu, T. Zhang, C. Grigorescu, H. J. Trodahl, L.Tortel, Appl. Surf. Sci. **247**, 139 (2005).
[12] M. Shima, T. Tepper, C.A. Ross, J. Appl. Phys. **91**, 7920 (2002).
[13] J. Hermann, A.L. Thomann, C. Boulmer-Leborgne, B. Dubreuil, M.L. de Giorgi, A. Perrone, A. Luches, I. N. Mihailescu, J. Appl. Phys. **77**, 2928 (1995).
[14] A. P. Caricato, G. Leggieri, A. Luches, A. Perrone, E. Gyorgy, I. N. Mihailescu, M. Popescu, G. Barucca, P. Mengucci, J. Zemek, M. Trchova, Thin Solid Films **307**, 54 (1997).
[15] J. Hermann, C. Dutouquet, J. Phys. D: Appl. Phys. **32**, 2707 (1999).
[16] K. V. Shalimova, Fizica Poluprovodnikov, Moskva, Energoatomizdat, 1985, p.392 (in Russian).
[17] I. Terasaki, Y. Sasago, K. Uchinokura, Phys. Rev. B, **56**, R12685 (1997).
[18] E. I. Rogacheva, S. G. Lyubchenko, M. S. Dresselhaus, Thin Solid Films **476**, 391 (2005).

*Corresponding author: luches@le.infn.it